SESSION I: THE NATURE OF THE DATA

Julius London presented a "tutorial overview" which began with a display the locations of total ozone stations (Fig. 1) and of stratospheric ozone samp lings (Fig. 2). The samplings are largely concentrated in three areas--Japan, Europe, and India. Approximately 75% of the total ozone measurements are made with Dobson instruments which offer the best international measurements. If th are well cared for and well calibrated, their accuracy is on the order of a

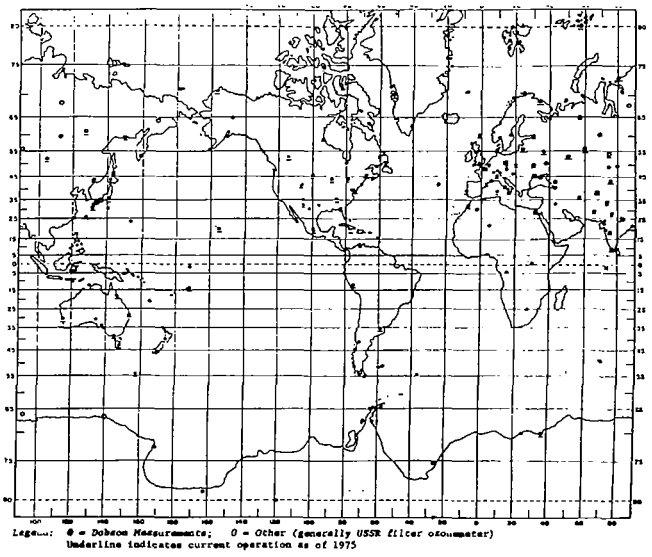

Figure 1. Location of Total Ozone Stations (1957-1975)

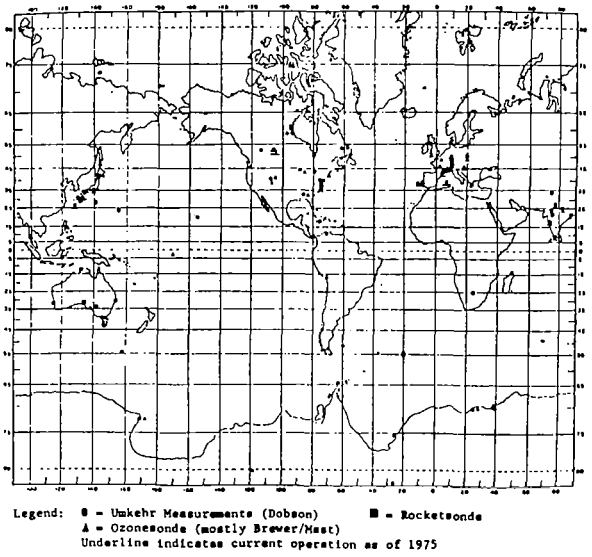

Figure 2. Observations of Stratospheric Ozone (1957-1975) (non-satellite)

few percent. Long period observations made with the same instrument have "relatively good" reproduction and reliability. The remaining 25% of the world's observations are made with filter instruments which were very noisy until the USSR improved them substantially in 1969. "Now," London said, "they are noisy rather than notoriously noisy."

Plotting the available data produces a picture of global distribution of total ozone (Fig. 3) that shows an equatorial minimum and an increase toward the polar regions. These features of the ozone distribution are both well-known. Variations in total ozone amount depend on season and latitude. This can also be seen in variance data from individual stations (Fig. 4).

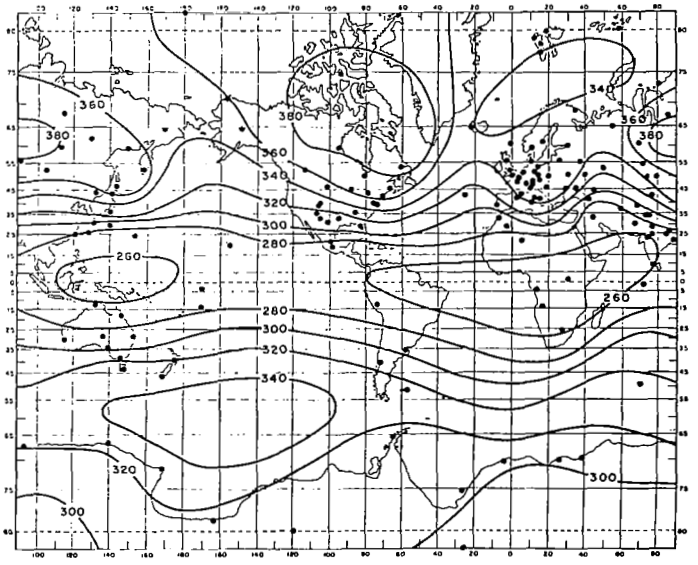

Figure 3. Distribution of Total Ozone for the Period 1957-1975 (m atm-cm)

Although the total ozone pattern is similar in both hemispheres, the northern hemisphere has 3 to 10% more total ozone than the southern hemisphere, not a negligible amount, according to London.

In the stratosphere, the hemispheric difference is even more pronounced as mid-latitude eddy transport is stronger in the northern hemisphere than in the southern. The maximum ozone concentration that occurs in the lower stratosphere varies with latitude and season. (In the summer and at the equator, the maximum is higher than in the winter and at the poles.)

London noted the "close association" between total ozone distribution and pressure distribution in the atmosphere. High amounts of ozone are clearly associated with large scale troughs in pressure distribution.

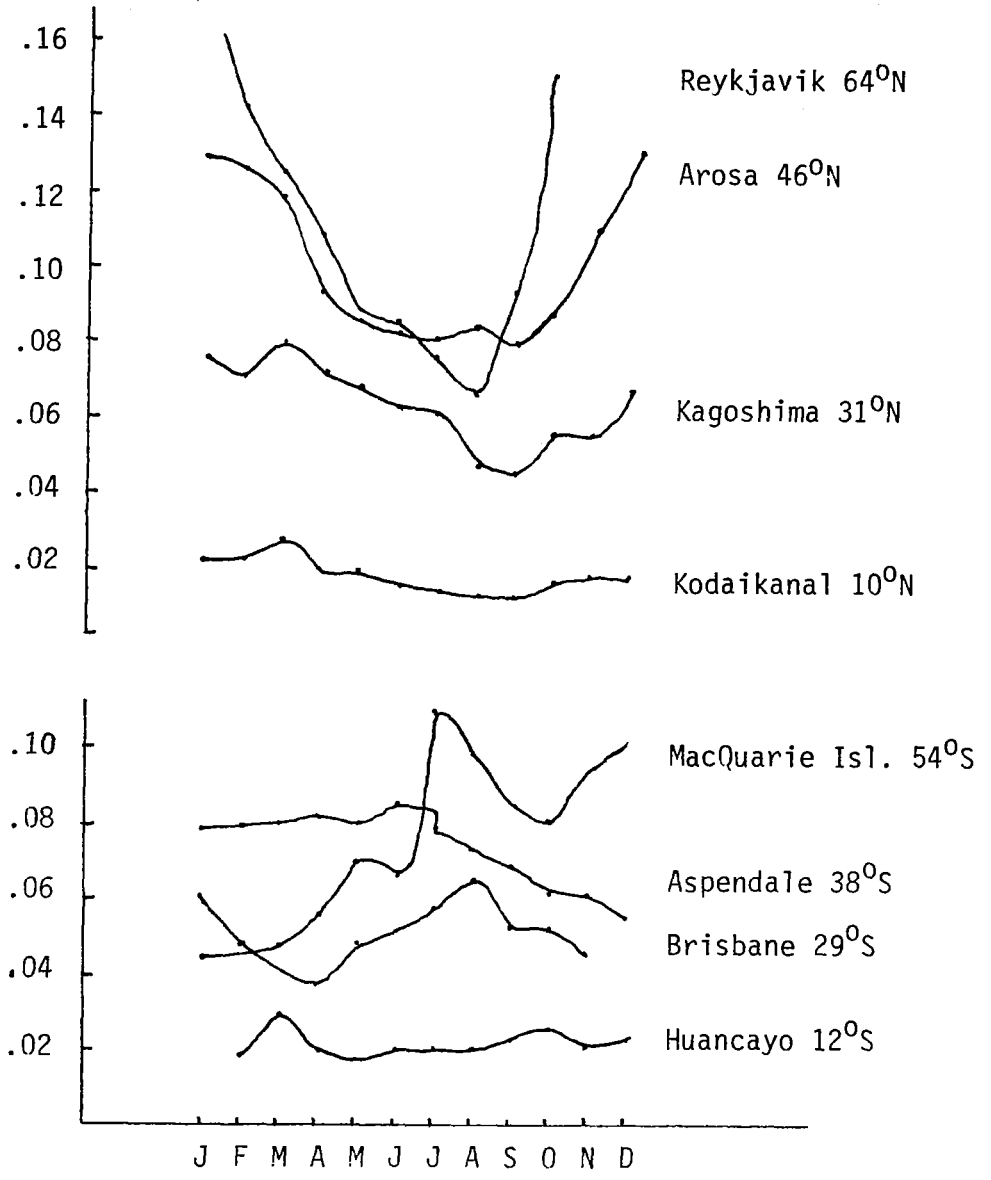

Figure 4. Seasonal and Latitudinal Variations in the Variance of Ozone Data

Displaying the average latitude seasonal variation (Fig. 5) shows the well-known spring maximum that is stronger in the northern hemisphere than in the southern. This spring maximum is also delayed a month in the south, a fact that London said was "more evidence of the relationship between ozone concentration and circulation" because it reflected the longer relaxation time in terms of the atmospheric circulation.

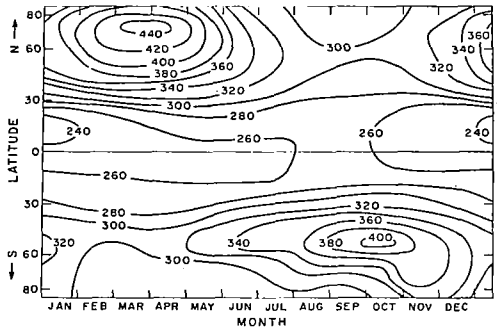

Figure 5. Average Latitude Seasonal Variation of Total Ozone

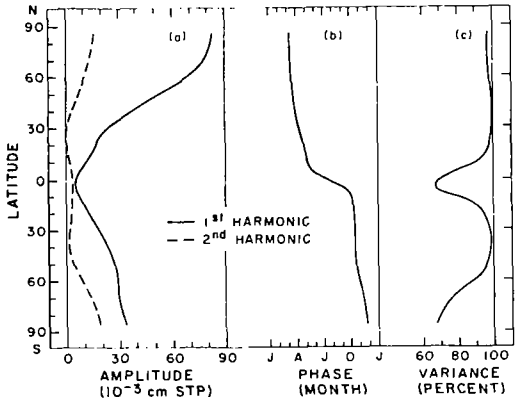

Figure 6. Latitudinal Distribution of the Harmonic Parameters of the Ozone Variation

To further reinforce his point that the variance of total ozone concentration is very like the behavior of the lower stratosphere and therefore the result of meteorological parameters, London fitted the mean monthly latitude values of ozone to the first harmonic (annual cycle) and second harmonic (phase) of the annual ozone variance (Fig. 6). Four different comparisons of these data (Fig. 7) then further supported his thesis.

Several statistical scientists commenting on their own efforts to smooth out the seasonal variance noted that: the variance of the reciprocals is less than that of the Dobson data; and nothing really stabilizes the variance although the reciprocal is better than the logarithm.

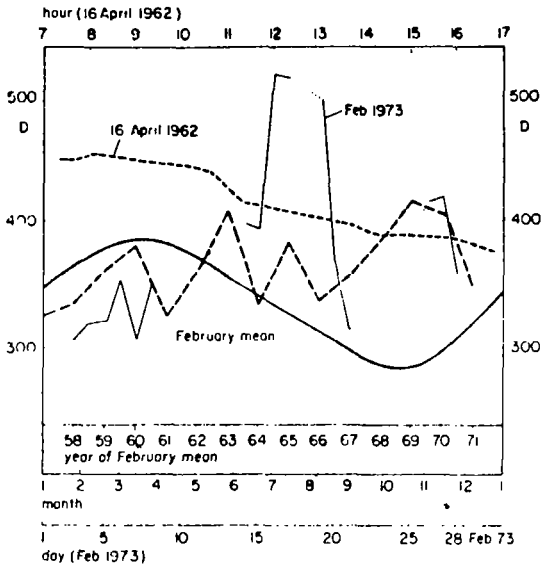

Figure 7. Comparison between the seasonal variation (monthly mean values) (———), the day-to-day changes within 1 month (February 1973), given by daily mean values (———), possible variation within 1 day (16 April 1962, single readings) (- - - - -), and the differences between mean values of the same calendar month (February) from year to year) (— — —).

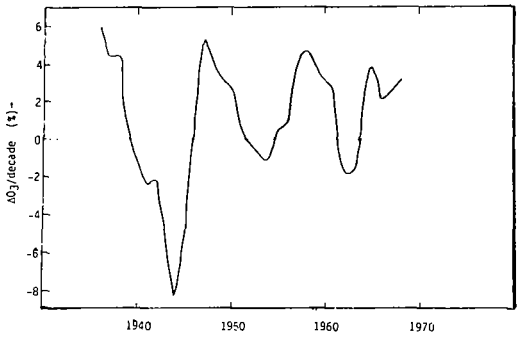

Figure 8. Ten Year Running Trend, Arosa, 1932-1973 (monthly means)

London then presented data from a single station, Arosa, Switzerland, where total ozone measurements have been made since 1926. These data (Fig. 8) indicate a long-term change of 6%, about half the standard deviation.

Walter Komhyr presented detailed information about Dobson measurements and the various algorithms used to calculate total ozone. The Dobson spectrophotometer (Fig. 9) takes in light from the direct sun or the zenith sky. The measurement principle requires measuring the ratio of intensities of solar radiation I/I' at pairs of wavelengths, λ and λ' (Fig. 10).

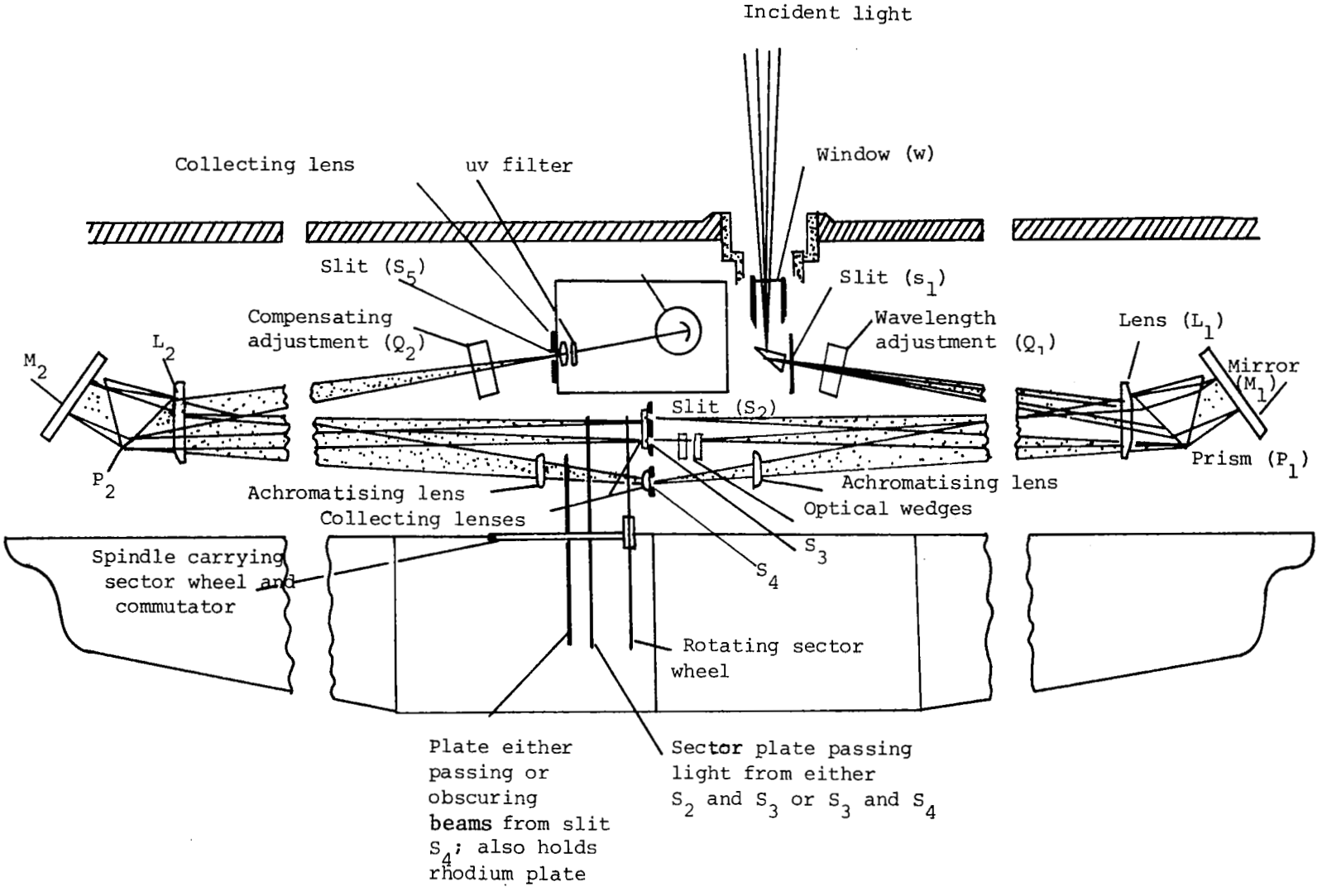

Figure 9. The Optical System

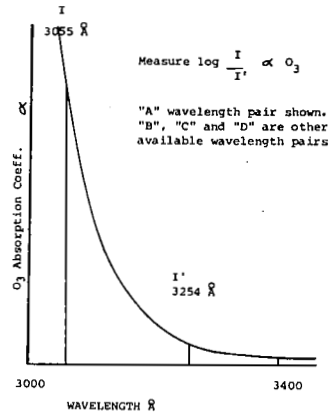

Figure 10. Ratio of Intensities of Solar Radiation I/I' at Pairs of Wavelengths, λ and λ'

Total ozone x is then calculated from the following equation:

$$x = \frac{L_0 - L - (\beta - \beta')mp/p_0 - (\delta - \delta')\sec Z}{(\alpha - \alpha')\mu} \qquad (1)$$

where $L = \log(I/I')$;

L_0 is the value of L at the top of the atmosphere;

α and α' are ozone absorption coefficients;

β and β' are molecular scattering coefficients;

δ and δ' are particle scattering coefficients;

μ is the slant path of light through the ozone layer;

m is the air mass;

p and p_0 are mean station pressure and mean sea level pressure, respectively;

and Z is the solar zenith angle.

The ozone absorption coefficients used before 1956 were 36% different from those currently set by the International Ozone Commission (Fig. 11).

Designation of Wavelength Pair		Mean Wavelength A.U.	Equivalent Instrument Slit Widths A.U	Atmospheric Scattering Coefficients (Rayleigh Cabannes formula)		Ozone Absorption Coefficients		
						Adopted for Use July 1, 1957*	Adopted for Use January 1, 1968**	
λ / λ'		λ / λ'	λ / λ'	β / β'	$\beta - \beta'$	α / α'	$\alpha - \alpha'$	$\alpha - \alpha'$
A	Short / Long	3055 / 3254	9 / 30	0.491 / 0.375	0.116	1.882 / 0.120	1.762	1.748
B	Short / Long	3088 / 3291	9 / 30	0.470 / 0.357	0.113	1.287 / 0.064	1.223	1.140
C	Short / Long	3114.5 / 3324	9 / 30	0.453 / 0.343	0.110	0.912 / 0.047	0.865	0.800
D	Short / Long	3176 / 3398	9 / 30	0.417 / 0.312	0.104	0.391 / 0.017	0.374	0.360
C'	Short / Long	3324 / 4536	30 / 15	0.343 / --	--	0.047 / nil	0.047	
AD					0.012		1.388	1.388
BD					0.009		0.849	0.780
AC					0.006		0.897	0.948
CD					0.006		0.491	0.440

*From July 1, 1957, the values of α are based on 1953 results of Vigroux for -44°C, which are about 36% smaller than the values of Ny and Choong used previously.

**Based on coefficients remeasured by Vigroux in 1967 as well as on atmospheric measurements, and recommended for use by the IAMAP.

Figure 11. Dobson Spectrophotometer Wavelengths and Constants

Solution of equation (1) involves dealing with the usually unknown term $(\delta - \delta')$. In practice, therefore, observations are made on double pair wavelengths in which case the particle scattering term becomes $(\delta - \delta')_1 - (\delta - \delta')_2$. To a good approximation, this quantity is assumed to equal zero. The equation for computing ozone using two wavelength pairs is

$$x_{12} = \frac{[(L_o-L)_1-(L_o-L)_2]-[(\beta-\beta')_1-(\beta-\beta')_2]mp/p_o-[(\delta-\delta')_1-(\delta-\delta')_2]\sec Z}{[(\alpha-\alpha')_1-(\alpha-\alpha')_2]\mu} \quad (2)$$

The most commonly used wavelength pairs are the A and D pairs and this equation is

$$x_{AD} = \frac{(L_o - L)_1 - (L_o - L)_2}{1.388\mu} - \frac{0.012mp}{\mu p_o} \quad (3)$$

Values for L, β, β', α, α', μ, m, p and p_0 are obtained using laboratory or other techniques. Calibration, i.e., measurements on direct sun, are needed to obtain L_0. The following equations describe the procedure for calibrating Dobson ozone spectrophotometers on an absolute scale.

Method 1. (Langley Plots). For observations made on clear days when $(\delta - \delta') \simeq 0$, equation (1) can be rewritten

$$L + (\beta - \beta')mp/p_0 = -(\alpha - \alpha')\mu x + L_0 \qquad (4)$$

which is linear in μ of the form $y = a\mu + b$ provided that x remains constant during the observing interval. By plotting $L + (\beta - \beta')mp/p_0$ against μ (for $0 \leq \mu \leq 3.2$) and fitting a line to the data, the slope is $a = -(\alpha - \alpha')x$ and the intercept is $b = L_0$. In this manner the extra-terrestrial constant, L_0, is determined for the instrument.

Method 2. (Slope Method). Equation (1) can also be written

$$L_0 - L - (\beta - \beta')mp/p_0 = (\alpha - \alpha')\mu x + (\delta - \delta') \sec Z \qquad (5)$$

Let L_0^* be the assumed approximate value of L_0, L_0 be the true value, and define $S = L_0 - L_0^*$. Then the equation

$$\frac{L_0^* - L - (\beta - \beta')mp/p_0}{\mu} = \frac{-S}{\mu} + (\alpha - \alpha')x + (\delta - \delta')\frac{\sec Z}{\mu} \qquad (6)$$

is linear in $1/\mu$. Plotting the left hand side of equation (6) against $1/\mu$ gives the slope $a = -S$, and the intercept is $b = (\alpha-\alpha')x + (\delta-\delta')$ for $\sec Z \simeq \mu$. The estimate of S is then used to correct the estimated L_0 value.

The primary standard Dobson spectrophotometer (instrument #83) was used as a reference instrument for a World Meteorological Organization-sponsored International Comparison of Dobson Ozone Spectrophotometers Meeting held in Boulder, Colorado, August 8-19, 1977. Regional secondary standard instruments from Australia, Canada, East Germany, Egypt, Japan, the United Kingdom, and India were compared with reference instrument #83.

A summary of similar instrument comparisons held in the past was presented by Komhyr (Fig. 12).

1. Hungary, 1969:

5 Eastern European Dobson instruments compared

2 groups insts. $\Delta O_3 \sim 10\%$

Discrepancies exceeding 20%

2. Belsk, Poland 1974*:

Inst. No	ΔN_{AD}	Δx_{AD}, $x \simeq 0.300$ cm			% error in x		
		$\mu=1$	$\mu=2$	$\mu=3$	$\mu=1$	$\mu=2$	$\mu=3$
41	0.016	0.012	0.006	0.004	3.8	1.9	1.3
64	0.108	0.079	0.039	0.026	26.3	13.0	8.7
77	-0.023	-0.017	-0.008	0.006	-5.5	-2.8	-1.8
83*	0	0	0	0	0	0	0
84	0.056	0.040	0.020	0.013	13.5	6.7	4.5
96	0.002	0.001	0.001	0	0.5	0.2	0.1
101	0.018	0.013	0.006	0.004	4.3	2.2	1.4
108	0.025	0.018	0.009	0.006	6.0	3.0	2.0
110	0.051	0.037	0.018	0.012	12.3	6.1	4.1
112	-0.024	-0.017	-0.009	-0.006	-5.8	-2.9	-1.9

*Spectrophotometer No. 83 was the reference instrument for the comparisons.

Figure 12. Results of Past Dobson Instrument Comparisons

Komhyr then presented data on additional absolute calibrations of U.S. standard spectrophotometer #83 that were made in 1962 and 1972. He also presented an analysis of the data which illustrated a method whereby possible variations in L_o values for the A, C, and D wavelength pairs may be detected. Such variations, for example, may occur with variations in sunspot numbers.

Komhyr concluded his presentation by examining the effect of possible changes in L_o with time on the accuracy of ozone measurements. He examined three cases:

Case 1: Single pair wavelengths A, B, C, D

$$x = \frac{L_o - L - (\beta-\beta')\, mp/p_o - (\delta-\delta')\sec Z}{(\alpha-\alpha')\mu}$$

$$\Delta x = \frac{\Delta L_o}{(\alpha-\alpha')\mu} \quad \text{where} \quad x_{true} = x_{meas.} + \Delta x$$

$\therefore$ If L_o increased during the 1960's, measured O_3 amounts were too low.

Assume:

$$\Delta L_{o\ 1976-1962} = 0.015 \text{ and } x = 0.300 \text{ cm.}$$

Then using:

$$\Delta x_A = \frac{0.015}{1.748\mu} \qquad \Delta x_C = \frac{0.015}{0.800\mu} \qquad \Delta x_D = \frac{0.015}{0.360\mu}$$

% Error in x			
μ \ $\lambda\lambda$	A	C	D
1	2.9	6.2	13.9
2	1.4	3.1	7.0
3	1.0	2.1	4.6

Case 2: Double pair wavelengths AD, CD

$$x_{AD} = \frac{L_{oA} - L_{oD} - L_A - L_D - [(\beta-\beta')_A - (\beta-\beta')_D]\, mp/p_o}{[(\alpha-\alpha')_A - (\alpha-\alpha')_D]\,\mu}$$

$$\Delta x_{AD} = \frac{\Delta L_{oA} - \Delta L_{oD}}{[(\alpha-\alpha')_A - (\alpha-\alpha')_D]\mu} = \frac{\Delta L_{oA} - \Delta L_{oD}}{1.388\ \mu}$$

Assuming that for the time interval 1962 to 1976

$$\Delta L_{oA} = 0.0154 \qquad \Delta L_{oD} = 0.0141 \qquad x = 0.300$$

$$\Delta x_{AD} = \frac{0.0013}{1.388\ \mu}$$

	% Error in x_{AD}
$\mu = 1$	0.3
$\mu = 2$	0.2
$\mu = 3$	0.1

Komhyr pointed out that if it is assumed that solar irradiance variations occur exponentially in the uv region of the solar spectrum, then errors in total ozone measurements resulting from L_o variations are insignificant when observations are made on double pair wavelength such as the AD pair which is the usual practice. However, observations made on single pair wavelengths could be significantly in error.

Case 3: CC' Observations

These are ozone observations made on the zenith sky using C wavelengths.

For $\Delta L_{oC} = 0.015$ and $x = 0.300$

	% Error in $x_{CC'}$
$\mu = 1$	4.0
$\mu = 2$	2.7
$\mu = 3$	2.0

Thus the errors in CC' observations due to solar intensity variations in the uv region of the solar spectrum can be appreciable.

Reid Basher then discussed systematic errors in Dobson measurements. He pointed out that the measurements are always in error to some extent, as a result of such things as aerosol scattering character, other atmospheric absorbing species, stratospheric temperature, instrument temperature, solar zenith angle, and solar spectral irradiance, but he noted that only those with long-term periodicities are important.

Instrument-related errors can be controlled by regular, rigorous calibration, but, in practice, this may be difficult, and not all errors will be known or appreciated. Atmosphere-related errors - attenuation by aerosols, absorption by other species such as SO_2 and NO_2, dependence of ozone absorption on temperature, and variations in the effective mean height of the ozone layer - can conceivably have long-term periodicities. For example, atmospheric particulate loading rises sharply with volcanic activity and decays with a relatively long half-life. These variable error sources will probably need to be monitored simultaneously in order to attain a high ozone trend detectability.

Basher selected as an example the case of atmospheric aerosols, particulates, and absorbers, explaining as follows:

Since the measurement between a pair of wavelength bands is a differential one, only relative effects are important, e.g.:

$$\log \frac{I_1}{I_2} = \log \frac{I_{o1}}{I_{o2}} - \mu X (\alpha_1 - \alpha_2) - m (\beta_1 - \beta_2) - \sec Z (\delta_1 - \delta_2) - (\gamma_1 - \gamma_2)$$

measurement; extraterrestrial constant; ozone; molecules; aerosol; other

Consider the effect of aerosol attenuation. If the effect is spectrally flat, $\delta_1 = \delta_2 = \delta(\lambda_0)$, it is eliminated directly within a band-pair measurement. If it is spectrally linear, $\delta_1 = \delta(\lambda_0) + g_1(\lambda_0 - \lambda_1)$, a third wavelength band or second band-pair is needed to eliminate the error.

For a quadratic dependence, $\delta_1 = \delta(\lambda_o) + g_1(\lambda_o-\lambda_1) + g_2(\lambda_o-\lambda_1)^2$, four wavelengths or three band-pairs are needed to eliminate the error. The standard Dobson measurement, X_{AD}, is a two band-pair measurement and thus deals effectively with spectrally linear effects (due to aerosols or other absorbers), but it will be in error if the effects are spectrally non-linear (Fig. 13).

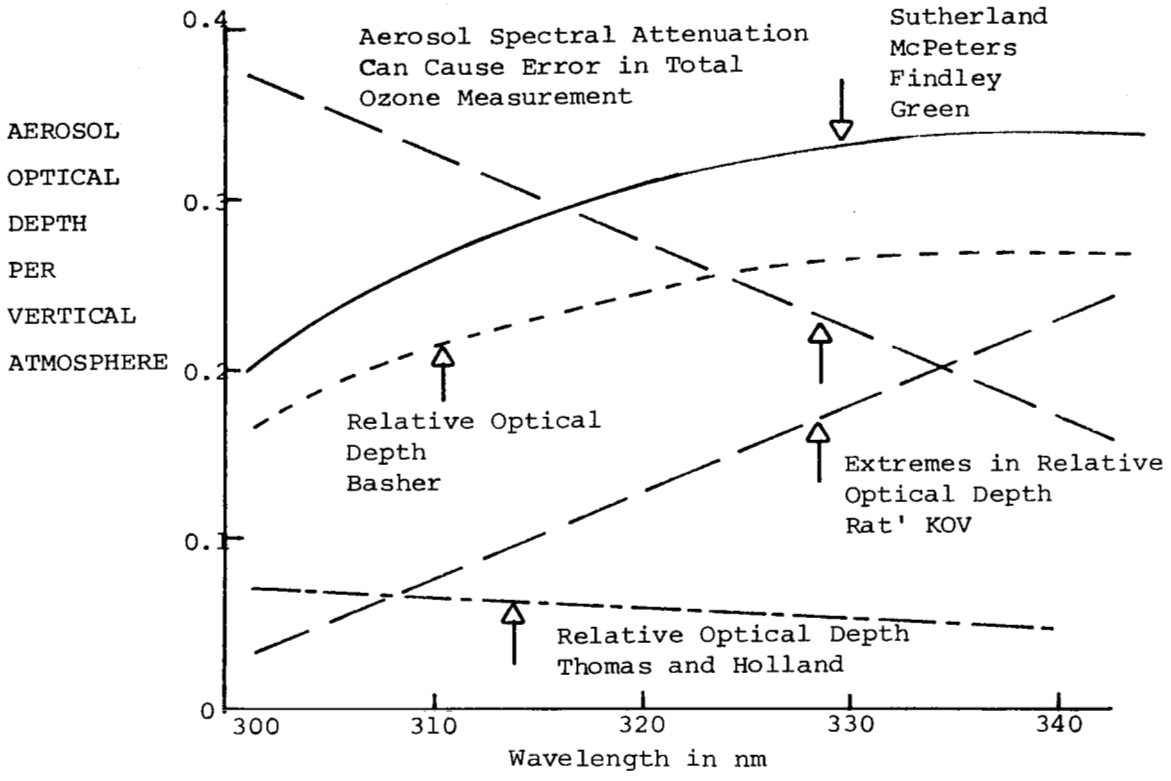

Figure 13. Atmospheric Aerosol and Total Ozone Measurement

Experimental measurements of atmospheric extinction indicate that sometimes there are significant spectral nonlinearities, with $g_2 \sim 4 \times 10^{-5}$, and consequent errors in X_{AD} of 5%. There is no firm agreement on this problem, since the experimental determination of g_2 is not very accurate, and theoretical calculations indicate that rather unusual types of aerosols are needed to produce the nonlinearities. The effect might well be due to an absorbing species.

One species which does absorb in the uv is NO_2. Fortunately, its absorption spectrum is reasonably linear so that its error component is largely eliminated by the double wavelength pair X_{AD} measurement. For a single wavelength pair, though, errors of many percent can arise where NO_2 concentrations are high, e.g. 40 ppb averaged over an atmospheric column. Typical values are 1 - 10 ppb, according to Basher. Further study is needed to assess the spectral non-linear extinction of aerosols and atmospheric trace species, as well as the long-term variability of the spectral character.

Basher then discussed a model of stray light (Fig. 14) that indicates a possibility of errors of several percent in the Dobson instrument, "always an underestimate." The error arises from the interaction of instrument and atmosphere, and is dependent on the instrument's sensitivity to the stray light, as well as the solar zenith angle and the atmosphere's ozone content. The instrument dependence can change slowly with time so a regular monitoring or correction of stray light is needed to avoid giving the appearance of long-term change in ozone. However, Basher concluded, the dependence of the stray light error on zenith angle and ozone itself simply adds an extra amplitude to the already existing yearly cycle term and is thus of no consequence.

Examining the case of calibration errors, Basher noted that calibration basically consists of ensuring constancy in the wavelengths of the bands and determining each band-pair's relative spectral output in the absence of the atmosphere, that is, determinining extraterrestrial constants. The first part involves simply a comparison with some stable wavelength standard. From the point of view of trend detection it is desirable to do this at least once a year. Quite rough wavelength calibrations would even be acceptable if they were made frequently and the "roughness" were random. The second part of the calibration is probably the most difficult aspect of ground-based total ozone measurement. For such measurements the "absence of the atmosphere" can only be gained indirectly, and the field measurements involved are time consuming and give inconsistent results that reflect as much as several percent variation in ozone measurements.

Basher reinforced Komhyr's point that the solar near-ultraviolet relative spectral irradiance may not be constant. For trend analysis, extraterrestrial constants need to be constant but not necessarily accurate. The instrument component of the constants can be calibrated with standard lamps, although past experience has shown this to be no easy task. The measurement of the solar uv component of the extraterrestrial constants requires an extra-atmospheric instrument location. The stability of this calibrating instrument must be better than the suggested 0.3% per year sensitivity of the ozone

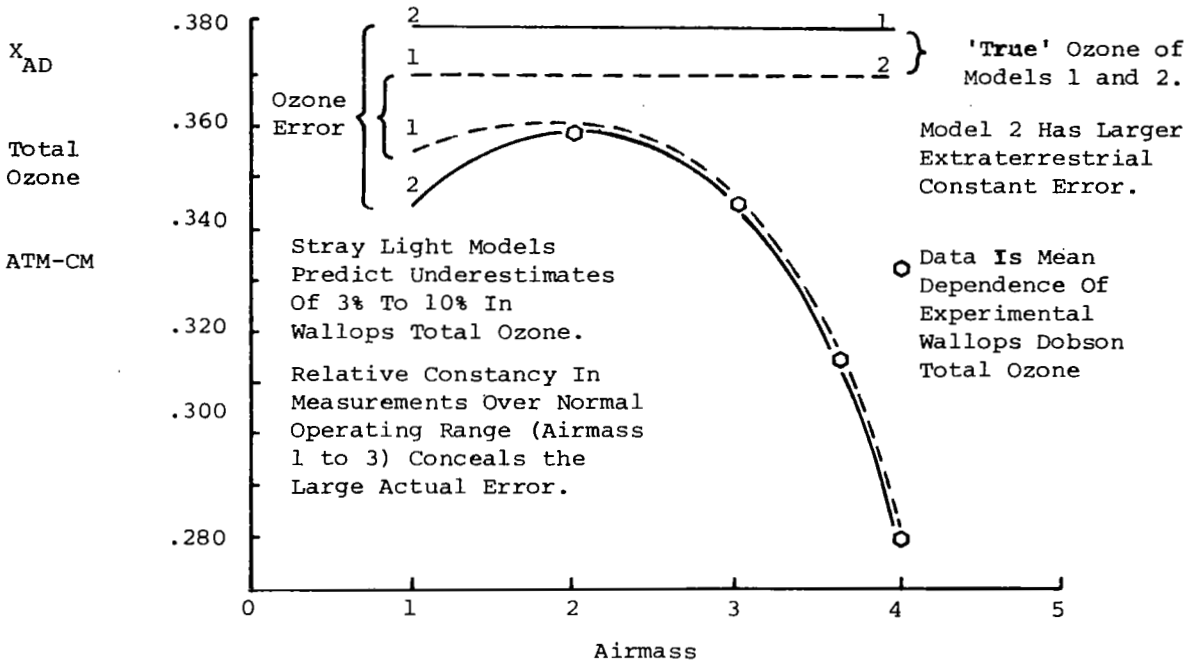

Figure 14. Model of Stray Light Error in Dobson Total Ozone

trend detection method; that is, it must be stable to less than 0.2% per year in relative spectral response. Moreover, there must exist means to independently verify the stability on a continual basis. Basher said, "The fact that at present such long-term stability is very difficult to achieve, even in the laboratory, should not completely discourage the consideration of preliminary remote space experiments."

In conclusion, Basher noted, "Our present lack of knowledge of the effects of aerosol attenuation and of other absorbers on the ozone measurement and our lack of certainty about the extra-terrestrial constants' constancy severely limit our ability to interpret measured trends as real ozone variation. It is quite possible that aerosols have no significant effect on X_{AD} total ozone, that the uv solar spectrum is particularly constant, and that the 0.3% per year detectability limit is meaningful. However, until we can prove these things we must accept a large uncertainty in trend detection results, probably more than 1% per year. Of course a good deal more study of systematic errors is needed."

Donald Heath next discussed satellite measurements of ozone using the nadir-looking BUV (Backscattered Ultra-Violet) instrument on NIMBUS 4,which was launched in 1970. This instrument is producing data at what Heath termed a cost of "about a dollar each over the life of the satellite, including original cost" (Fig. 15). NIMBUS G planned for 1978 as well as the TIROS N series may carry similar instruments.

The BUV instrument measures the ultraviolet solar radiation which is backscattered by the earth and its atmosphere and compares this, at varying wavelengths between 2550 and 3400 angstroms, to the incoming uv radiation (Fig. 16). The data are used to estimate both vertical profiles of ozone down to the 0.2 millibar level and total ozone. The data inversion technique requires a statistical quantity for P*, the pressure height of the maximum ozone level as a function of latitude and season. Balloon and rocket data help provide upper and lower first guesses (Fig. 17).

So far total ozone data have been released for the first year of the satellite's mission and these data are currently undergoing a revision based on improved calibration of the instrument.

"We need guidance to determine long term instrument performance," said Heath. He then went on to discuss the puzzle of knowing which Dobson instruments to use for ground truth. Integrating data over the whole globe, he compared BUV and Dobson measurements.

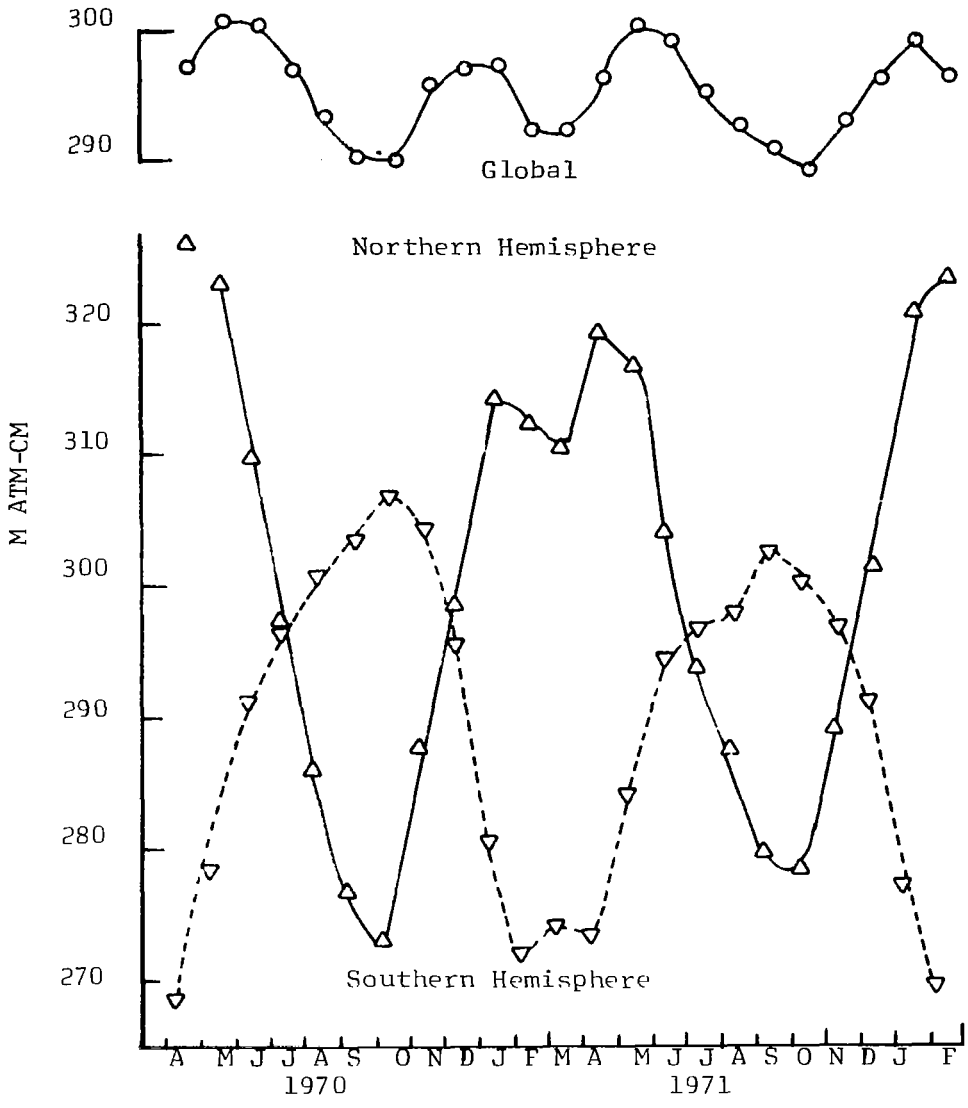

Figure 15. Ozone Monthly Mean

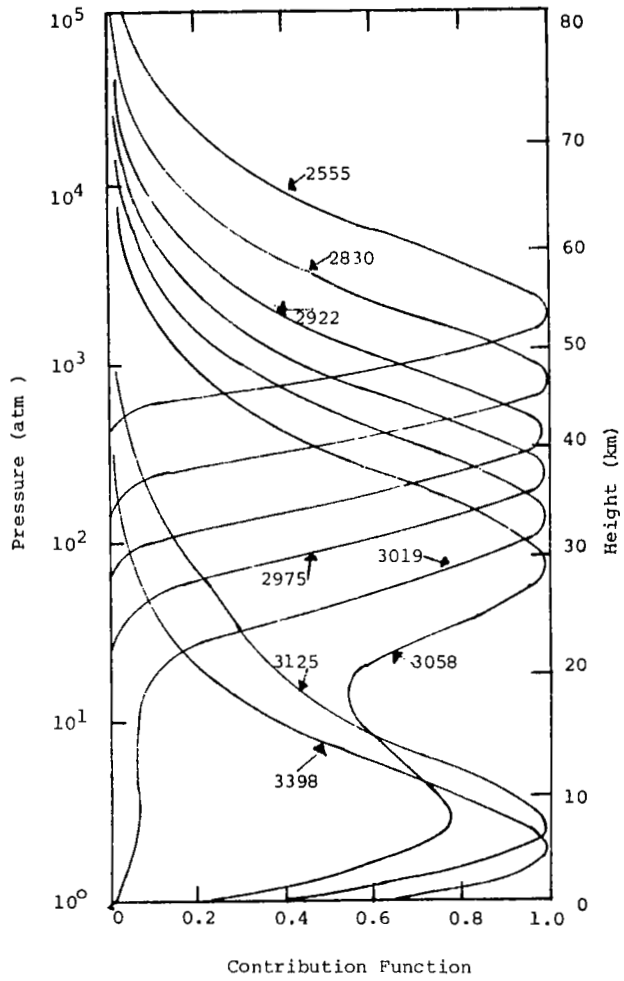

Figure 16. Effective Scattering Levels for Solar Radiation Scattered in the Nadir Direction of the Satellite for all Orders of Scattering (Solar zenith angle = 60°; Total ozone = 336 m atm-cm)

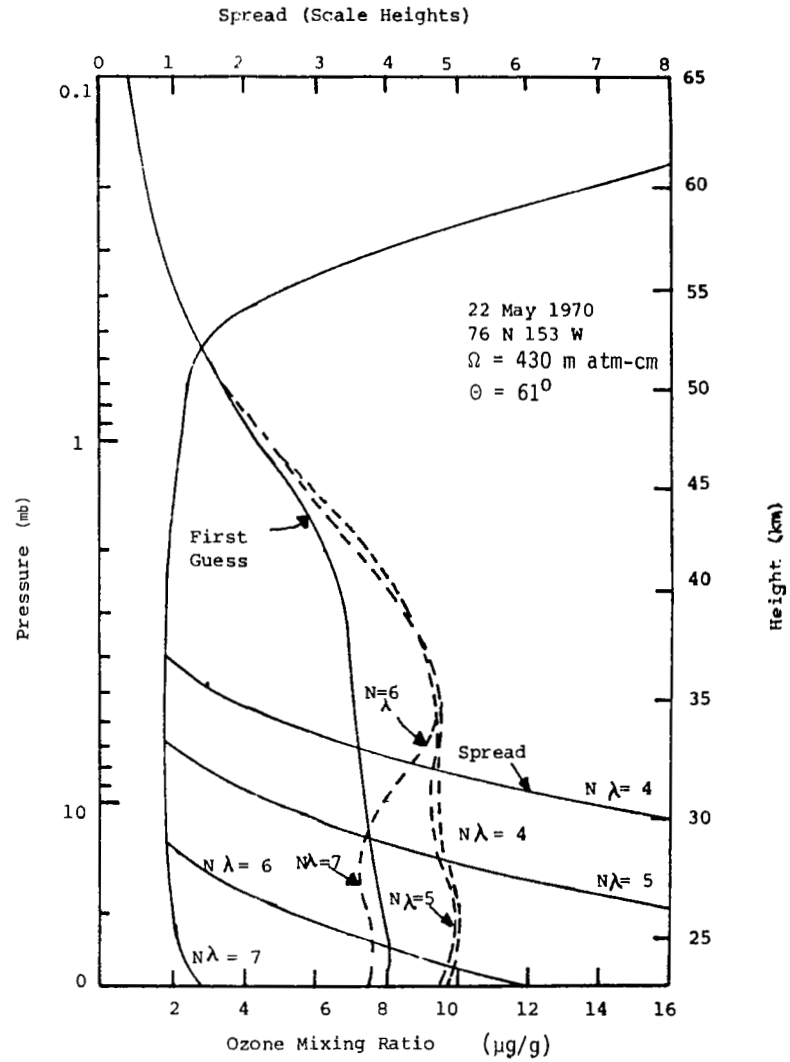

Figure 17. Balloon and Rocket Data

Figures 18 and 19 display two data sets from satellite observations. The massive solar proton event of August 4, 1972, is seen dramatically in a cavity in the ozone formed over the North Pole that persisted for at least two months. This same effect was not observed in the southern hemisphere, probably because it was winter and the ozone variability was very high.

Heath concluded that NASA's primary interest is in the stable high altitude observations where any effect of CFMs should show up. Figure 20 shows NASA's March 1977 assessment of the percent change in ozone due to CFMs.

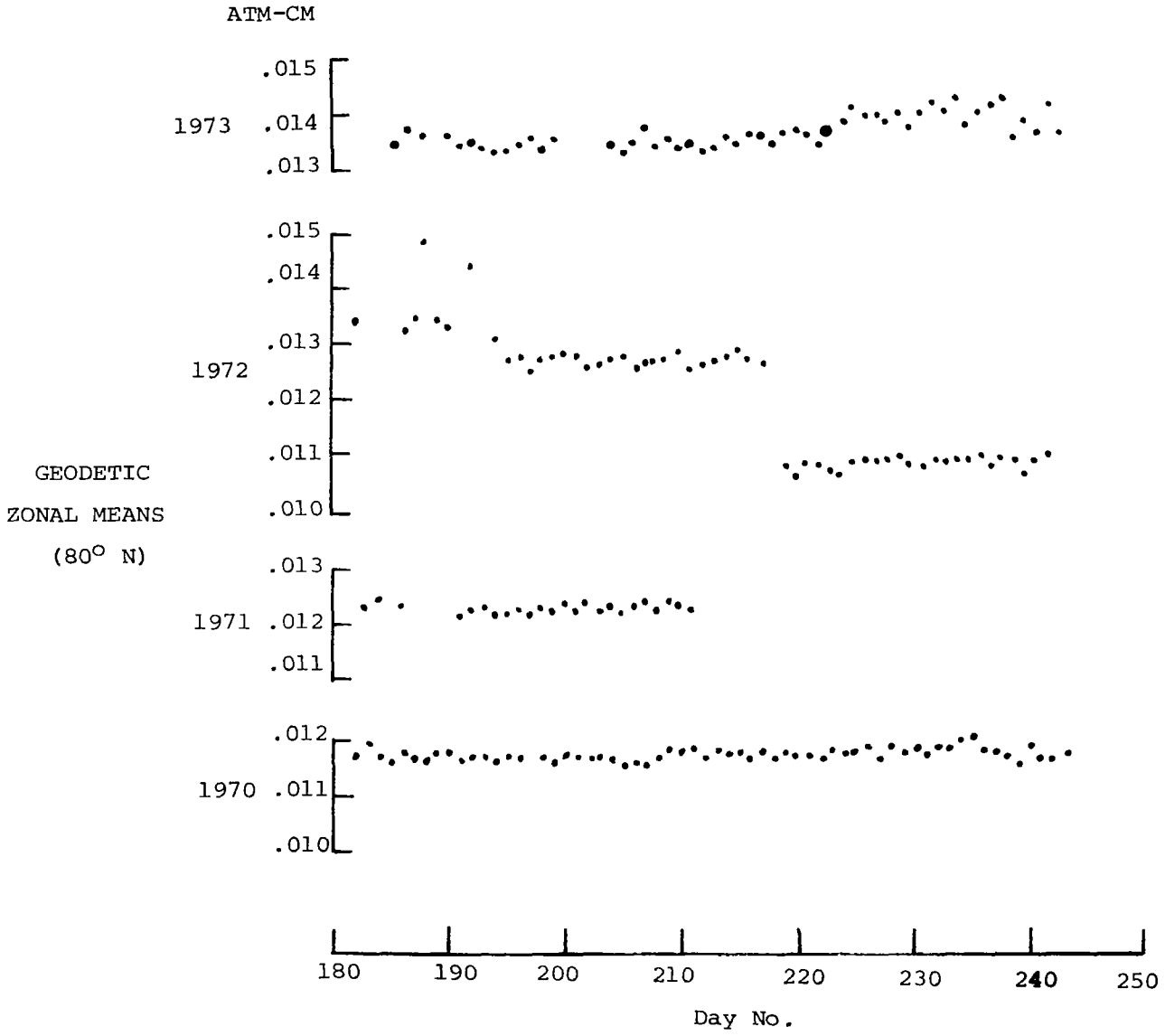

Figure 18. Geodetic Zonal Means (80° N)

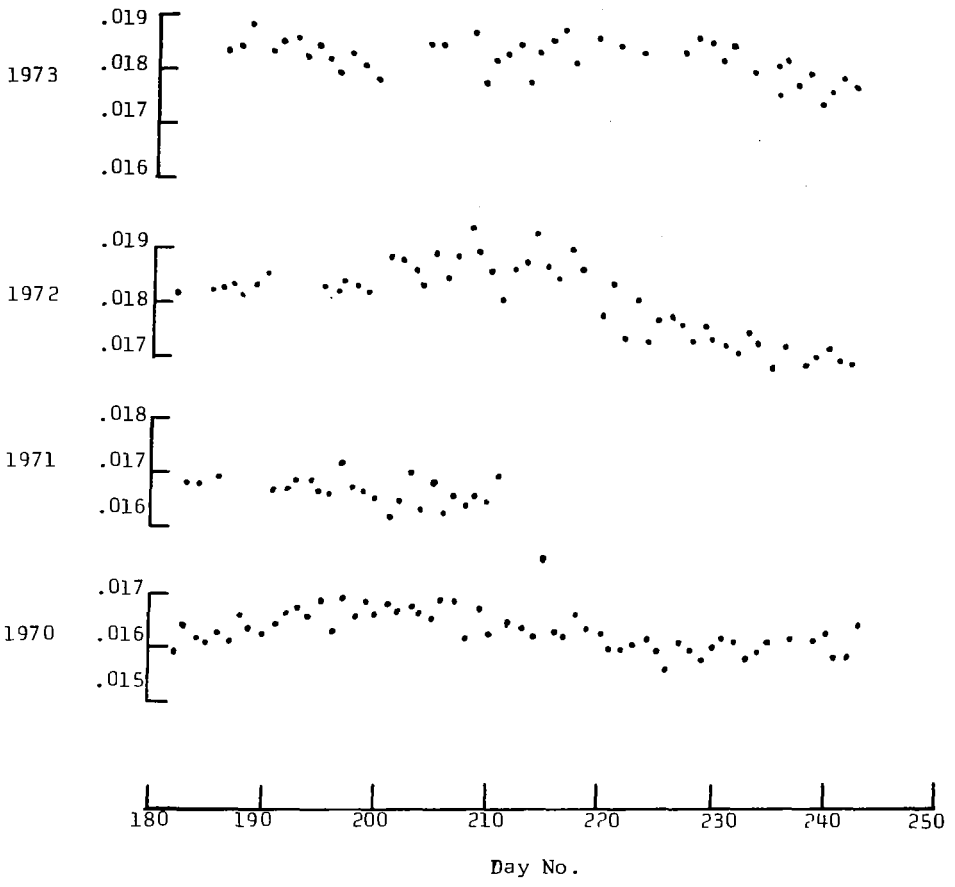

Figure 19. Geodetic Zonal Means (0^{o})

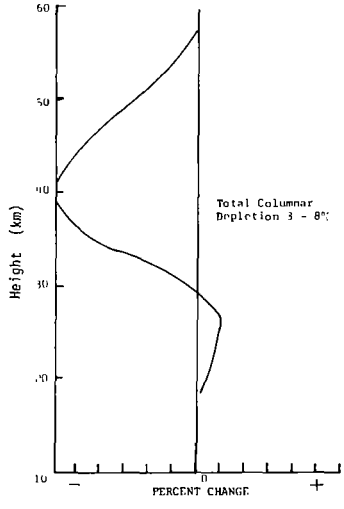

Figure 20. Depletion of Ozone due to CFMs, NASA Assessment, March 1977

John Gille briefly described his Limb Radiance Infrared Radiometer (LRIR) results with a special note on the difference between accuracy and precision. The LRIR receives radiation from a 200- to 300-km-long path through the atmosphere. Cold space behind the earth's limb eliminates any problems with background radiation and the ray path eliminates interference from any lower atmospheric regions. The LRIR produces vertical ozone distributions from 15 to 55 kms, as well as temperature distributions (15 to 70 km). Water vapor profiles are expected in the future.

Gille stated that the LRIR accuracy is comparable to that of other instruments including the optical rocketsonde, the chemiluminescent sonde, and the balloon ozonesonde. As to precision, he noted that the LRIR instrument could get a reading every 25 km or 12 to 15 profiles every 4° of latitude. The standard deviation for a single profile is a function of altitude, but ranges from about 1% at 30 km to 3% at 40 km and 10% at 48 km. He noted that comparisons between LRIR and Limb Infrared Monitor of the Stratosphere (LIMS), to be launched in 1978, would provide a very sensitive test of variations at 40 km. For accuracy, he noted that the rms agreement with the chemiluminescent rocketsonde was 10%, about the stated accuracy of the rocket measurement.

James Lovill described the Air Force defense meteorological polar orbiting satellite which can send 68,400 observations a day to the Satellite Ozone Analysis Center (SOAC). Twenty-three Dobson stations in 13 countries have agreed to provide special ground truth measurements to the SOAC to use with the satellite data.

Detailing the measurement procedure, Lovill explained the instrument, its flow diagram, some specific instrument parameters, and the sensor scan geometry (Fig. 21). He then presented satellite readings (Fig. 22), contoured them over the globe (Fig. 23), and provided Arosa readings for July 1977 (Fig. 24) as an example of the ground truth measurements. He concluded his presentation with a display of correlation coefficients vs. distance for two sets of total ozone stations (Figs. 25 and 26).

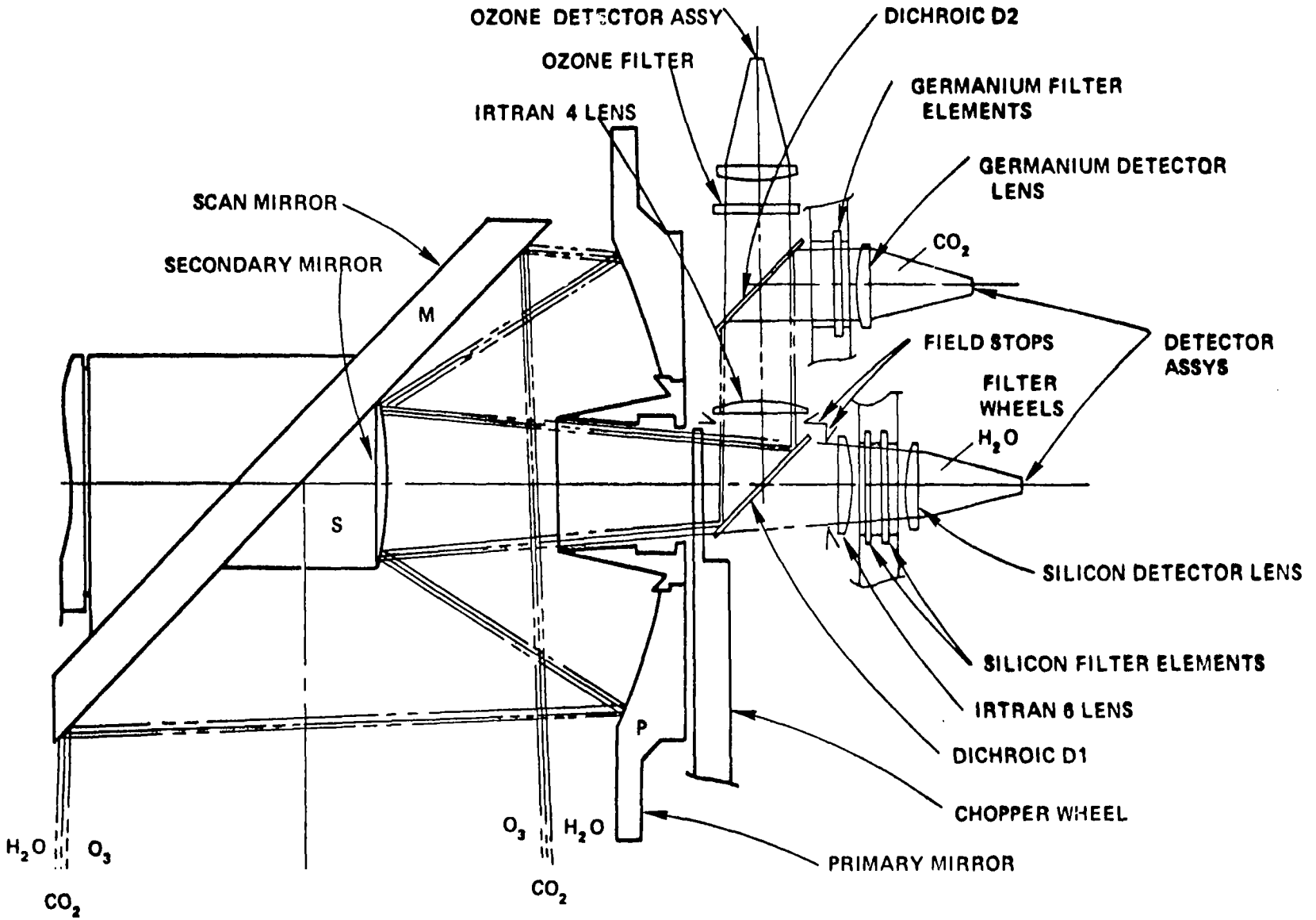

Figure 21. Optical Schematic of Ozone, Temperature and Water Vapor Sensor

April 19, 1969

70N	460	479	410	398	440	427	430	434	431	443	452	449	451	449	424	435	429	378	434
50N	397	413	352	367	420	351	389	400	371	403	422	399	384	361	334	370	390	349	381
30N	312	325	319	334	362	315	362	352	306	325	317	299	300	248	297	314	330	333	319
10N	252	254	256	251	265	257	317	290	263	267	251	265	260	241	265	267	307	295	267
10S	245	242	239	236	237	237	296	273	259	255	238	260	261	260	249	268	289	261	255
30S	280	283	288	300	286	288	307	289	289	291	274	281	289	268	279	303	282	202	208
50S	333	334	326	327	322	351	320	290	333	350	349	364	350	362	338	316	324	345	335
70S	383	371	338	340	362	390	362	347	369	379	375	411	436	369	362	329	362	390	370
	170W	150W	130W	110W	90W	70W	50W	30W	10W	10E	30E	50E	70E	90E	110E	130E	150E	170E	MEAN

Figure 22. Satellite Readings

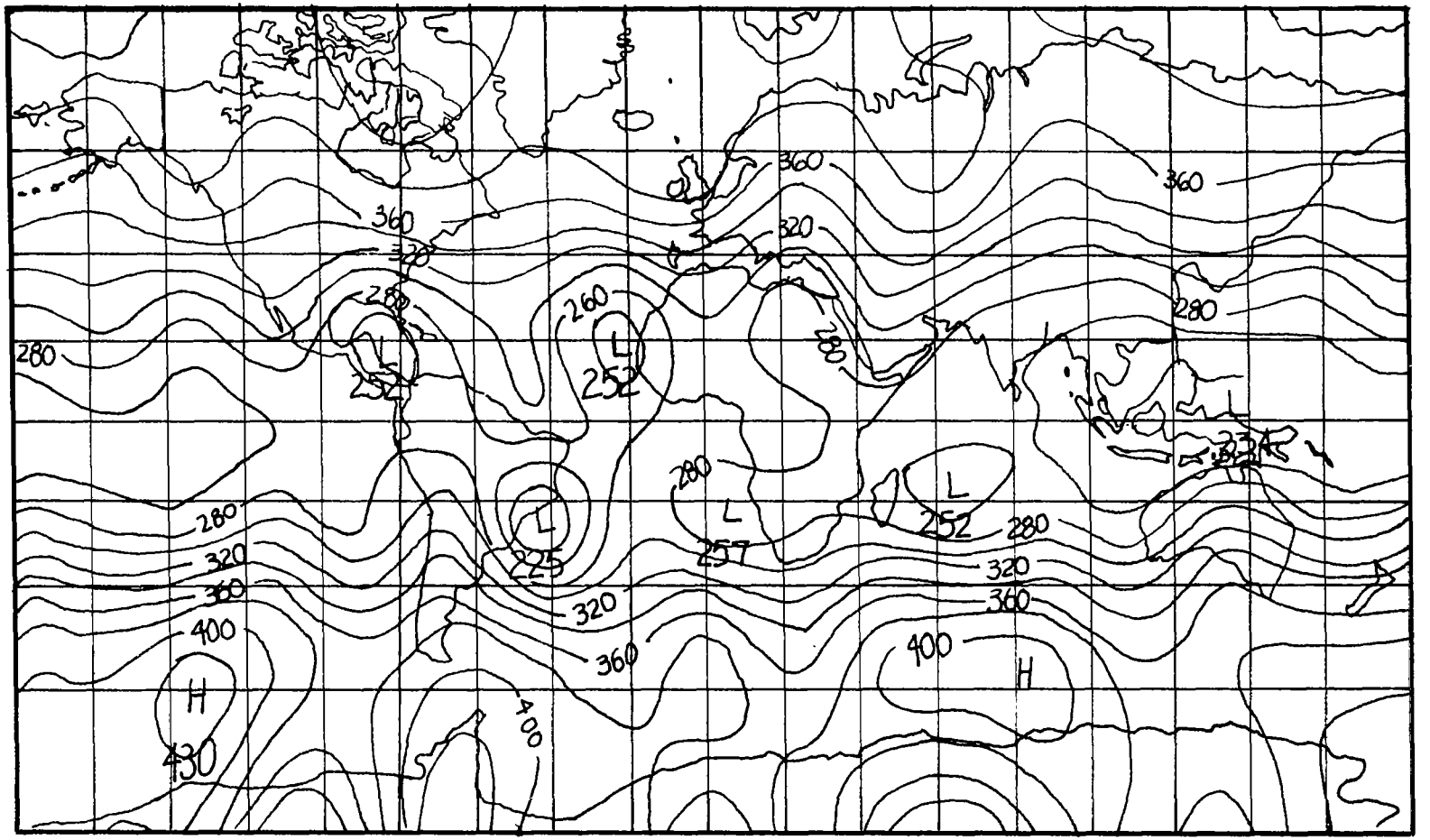

Figure 23. Satellite Readings Contoured Over the Globe

	D 15							GMT + 1h	D 101						
Day	TIME	$I_\odot$	C	TIME	$I_\odot$	AD		TIME	$I_\odot$	C	TIME	$I_\odot$	AD
11	7 46 30	4	351	7 47 30	4	345		7 48 30	4	340	7 50 30	4	347
	8 54 30	4	341	8 55 30	4	340		8 57 30	4	334	8 58 30	4	339
	10 24 30	4	345	10 25 30	4	342		10 27 30	4	333	10 28 30	4	344
	11 28	4	344	11 28 45	4	335		-	-	-	-	-	-
	11 30	4	343	11 30 45	4	336		11 32	4	329	11 32 45	4	337
	13 29	3-4	336	13 29 45	3-4	332		11 34	4	328	11 34 45	4	341
								13 31	3-4	327	13 35 15	3-4	339
12	7 04 30	4	303	7 05 30	4	302		7 07 30	4	292	7 08 30	4	299
	7 24 30	4	305	7 25 30	4	301		7 27 30	4	292	7 28 30	4	301
	7 47 30	4	304	7 48 30	4	304		7 50 30	4	295	7 51 30	4	303
	9 55 30	4	305	9 56 30	4	301		9 58 30	4	290	9 59 30	4	303
	11 10	4	301	11 10 45	4	301		11 14	4	290	11 14 45	4	303
	11 12	4	301	11 12 45	4	301		11 16	4	291	11 16 45	4	301
	11 51 30	4	305	11 52 30	4	300		11 54 30	4	292	11 55 30	4	301
	12 59 30	4	311	13 00 30	4	300		13 02 30	4	295	11 03 30	4	301
13	10 06 30	4	346	10 07 30	4	335		10 09 30	4	335	10 10 30	4	335
	11 10	3-4	345	11 10 45	3-4	333		11 12	3-4	333	11 12 45	3-4	334
14	8 27 30	3	336	-	-	-		8 25 30	3-4	328	8 26 30	3-4	329
	13 11	3	335	13 11 45	3	343		-	-	-	-	-	-
								13 13	3	341	13 14 45	3	344
								14 33	2-3	335	-	-	-
15	12 17	2-3	338	12 17 45	2-3	340		-	-	-	-	-	-
	12 55	3	345	12 55 45	3	345		12 55	3	337	12 55 45	3	343
	16 04	3	332	-	-	-		17 11	3	322	17 12 30	3	329
16	7 06 30	-4	327	7 07 30	-4	323		7 09 30	-4	317	7 10 30	-4	323
	7 25 30	4	331	7 26 30	4	326		7 25 30	4	319	7 26 30	4	325
	7 49 30	4	332	7 50 30	4	327		7 52 30	4	320	7 53 30	4	327
	9 32 30	4	341	9 33 45	4	333		9 36 30	4	328	9 37 30	4	344
	10 37	3-4	340	-	-	-		10 31 30	3-4	335	10 32 30	3-4	345
	11 43	4	344	11 43 45	4	338		-	-	-	-	-	-
	12 51 30	3-4	353	12 52 15	3-4	345		12 58	4	335	12 58 45	4	350
17	12 30 30	2-3	73.8	-	-	-		-	-	-	-	-	-

Figure 24. Arosa Readings for July 1977

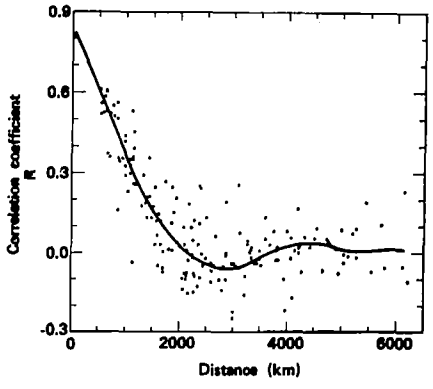

Figure 25. North American Total Ozone Stations
(Data Period: 1960-1975)

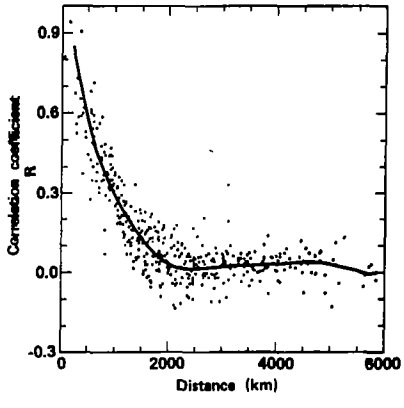

Figure 26. European Total Ozone Stations
(Data Period: 1960-1975)